Development of Semicontinuous Measurement System of Ionic Species in $PM_{2.5}$

Sang-Bum Hong,[*,†,a] Wonil Chang,[*,b] Chang-Hee Kang,[‡] and Jai H. Lee[†]

[†]*Advanced Environmental Monitoring Research Center (ADERC), Department of Environmental Science and Engineering, Gwangju Institute of Science and Technology (GIST), Gwangju 500-701, Korea. [*]E-mail: hong909@kopri.re.kr*
[‡]*Department of Chemistry and Research Institute for Basic Sciences, Cheju National University, Jeju 690-756, Korea*
Received December 2, 2008, Accepted May 12, 2009

A new method to semicontinuously determine $PM_{2.5}$ ionic species with a short time resolution is described in detail. In this system, a particle collection section (mixing part, particle collection chamber, and air/liquid separator) was developed. A Y-type connector was used to mix steam and an air sample. The particle collection chamber was constructed in the form of a helix coil and was cooled by a water circulation system. Particle size growth occurred due to the high relative humidity and water absorbed particles were efficiently collected in it. Liquid samples were drained out with a short residence time (0.08-0.1 s). The air/liquid separator was also newly designed to operate efficiently when the flow rate of the air sample was 16.7 L min^{-1}. For better performance, the system was optimized for particle collection efficiency with various types of test aerosols such as $(NH_4)_2SO_4$, NaCl, NH_4HSO_4, and NH_4NO_3. The particle collection efficiencies were almost 100% at different concentration levels in the range over 500 nm in diameter but 50-90% in the range of 50-500 nm under the following experimental conditions: 15 coil turns, a water flow rate for steam generation of 0.65 mL min^{-1}, and an air sample flow rate of 16.7 L min^{-1}. Finally, for atmospheric applications, chemical compositions of $PM_{2.5}$ were determined with a time resolution of 20 min on January 11-24, 2006 in Seoul, Korea, and the chemical characteristics of $PM_{2.5}$ ions were investigated.

Key Words: $PM_{2.5}$, Particle collection section, Semicontinuous measurement system

Introduction

Particles less than 2.5 μm in diameter ($PM_{2.5}$) in the atmosphere can play important roles in radiative forcing,[1] visibility degradation,[2] heterogeneous atmospheric chemistry,[3] and human health.[4] Indirectly, they act as cooling agents by increasing albedo and the lifetime of shallow marine clouds.[5] They also contribute to acidification and eutrophication of land and water resources via wet and dry deposition.[6]

As a result, much research has been conducted to examine these issues. In order to investigate the chemical characteristics of these particles, a reasonably short time resolution is essential since the particles changes their properties over a short time in the atmosphere.[1-8] However, the widely used filter methods cannot capture the rapid changes in the chemical compositions of particles owing to their relatively long sampling frequencies. In addition, these methods was reported to suffer from sampling artifacts such as reactions on filter media and loss of semi-volatile species during and after collection.[9] Recently, to overcome the drawbacks of the filter methods, a variety of semicontinuous measurement methods have been developed over the last decade.[10-16]

$PM_{2.5}$ in the atmospheric environment typically includes most of the total number of particles, surface area, and a large fraction of the mass. However, collection of particles in the range of 0.1-1.0 μm is not simple because particle removal mechanisms, such as diffusion and impaction, are least efficient in this regime.[17-18] Thus, an appropriate device needs to be developed to allow effective collection by utilizing a semicontinuous measurement system. Previous studies have suggested that such fine particles could be collected efficiently *via* impaction after increasing their size by water vapor saturation. Aerosol particles can take up water vapor and then grow to a certain equilibrium size, as the relative humidity (RH) reaches the deliquescence point. Hot steam has typically been injected to increase the RH in a system with small particles.

Simon and Dasgupta (1995) used a mixing chamber in the form of a circular tube connected with a short segment of gently curved PTFE tubing, where superheated steam (~ 300 °C) was introduced along with an aerosol sample at 10 L min^{-1}. The particles were further grown in a cooled stainless steel maze and then collected in a gas/liquid separator. The steam jet aerosol collector (SJAC) gathered the grown droplets in a cyclone at a sample flow rate of 20-60 L min^{-1} after mixing steam and an aerosol sample.[11] Concentration columns have typically been installed in ion chromatography systems due to their sensitivities. A prototype particle-into-liquid sampler (PILS), operating at a flow rate of 5 L min^{-1}, has been developed to rapidly speciate and quantify small liquid samples, without using a concentrator. Furthermore, an improved analyzer, operating at a flow rate of 16.7 L min^{-1}, was developed and used successfully in an airplane measurement campaign.[19-20]

In this study, a semicontinuous system to measure $PM_{2.5}$ ionic species was developed. In principle, our system is identical to the well established particle collection system described in previous reports.[11-12,14] However, the particle collection section (mixing part, particle collection chamber, and air/liquid separator) was specifically built and tested. In particular, a particle collection chamber was developed to not only induce

[a]present address : Korea Polar Research Institute, KORDI, Incheon 406-840, Korea. [b]present address : Department of Earth and Environmental Sciences, Korea University, Seoul 136-701, Korea

the size growth of small particles, but also to efficiently collect water-absorbed samples. This is an advantage of our system over that of previous ones. As a performance test, collection efficiencies using test aerosols, such as $(NH_4)_2SO_4$, NaCl, NH_4HSO_4, and NH_4NO_3, were conducted. Finally, field monitoring results for ionic species in $PM_{2.5}$ were also presented.

Experimental Section

Aerosol sampling and interference gas removal. In order to collect $PM_{2.5}$ and to remove acidic and basic gases in ambient air, were used a $PM_{2.5}$ cyclone (URG-2000-30 EH) with a 2.5 μm cutoff at a sample flow rate of 16.7 L min^{-1} and a denuder systems (URG-2000-30×242-3CSS) with a collection efficiency of 99% at a sample flow rate of 16.7 L min^{-1}. The denuders used in this system can effectively retain gaseous species, such as HNO_3, HNO_2, SO_2, and NH_3. Because the diffusion coefficients of gas molecules are typically four orders of magnitude larger than the smallest atmospheric particle, quantitative removal of gas molecules by diffusion is possible. Under laminar flow conditions and with a vertical deployment of the denuder tube, gravitational settling of aerosol particles can be avoided and the aerosol can be transmitted efficiently. The coating solution was prepared according to the use and maintenance manual for URG annular denuders.[21,22]

Particle collection section. Figure 1 shows a schematic diagram of the measurement system and Figure 2 displays important components of the particle collection section (mixing part, particle collection chamber, and air/liquid separator) made of Pyrex glass. The aerosol samples passing through the gas removal denuder tubes were introduced to a Y-connector mixing area, and then were mixed initially with hot water vapor (Fig. 2a). The flow direction of aerosol samples at a higher flow rate (16.7 L min^{-1}) than that of the water vapor (~ 0.75 L min^{-1}) was forced to change abruptly, to induce a turbulent flow of the air stream. This can enhance the rapid and efficient mixing of the steam and the aerosol, before water vapors condense on the wall surface of the mixing area. Water vapors cannot condense on an aerosol surface and thus cannot contribute to size growth once they are liquidized on another surface. The steam generator was specifically designed to produce homogeneous water vapor. Steam was produced in a stainless steel (SS) tube (ID 1/8", 12 cm) connected with a coil of SS tubing, through which distilled water was pumped; its temperature was controlled at ~ 110 °C.

The most prominent feature of our system was a particle collection chamber designed in a helix coil form, as shown in Figure 2b. Except for an 8 cm length at each end, the rest of the tube (Pyrex glass, 3 mm i.d.) was turned. Generally, a helix-type coil sampler is used to continuously collect soluble gaseous species with high Henry's law constants in online measurement systems,[23] but it was utilized to verify a particle collector in our system. This was surrounded by a jacket through which cooling water was introduced and a temperature close to 20 °C was maintained to increase the RH in it. After air samples were initially mixed with hot steam in the mixing area, they began to absorb water vapor while they passed

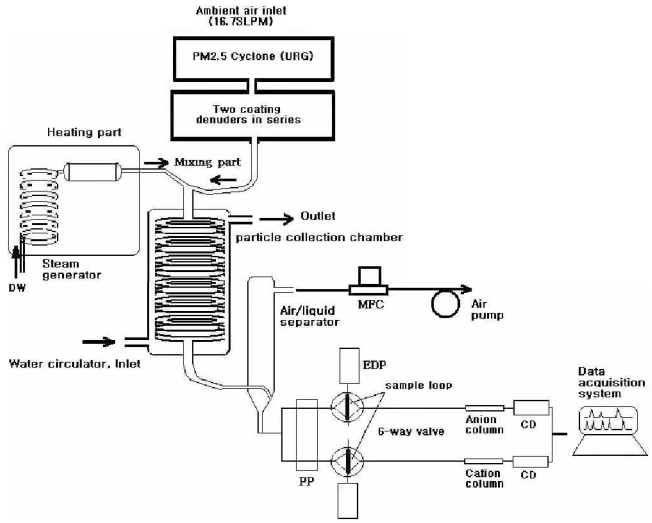

Figure 1. Schematic diagram of semi-continuous measurement system, consisting of denuders, a steam generator, a particle collection section (mixing part, particle collection chamber, and air/liquid separator), and IC system (DW; distilled water, MFC; mass flow controller, EDP; eluent delivery pump, PP; peristaltic pump, CD; conductivity detector).

through the particle collection chamber with a high RH. The sizes of particles increase due to the spontaneous absorption of water at RHs higher than the deliquescence relative humidity (DRH) and the masses of water-absorbed samples also increase significantly.[18,24-27] The RH in the chamber was ~ 300% under the following experimental conditions: an air sample flow rate of 16.7 L min^{-1}, 25 °C temperature of the ambient air with 60% RH, a flow rate of water for generating steam of 0.65 mL min^{-1}, and a 110 °C steam temperature. Water-absorbed particles can be impacted efficiently on the inner surface of the helix coil due to both an inertial force, enhanced by the increase in aerosol mass, and a centrifugal force, caused by movement through the curvature. As a result, the particles experience not only size growth, but also continuous collection in it. This is quite different from other particle collection sections in previous semicontinuous measurement systems. In the previous studies, the particle collection apparatuses were generally composed of a size growth chamber and particle collection device such as a cooled SS maze, a cyclone, or a single jet impactor.[11-12,14,19] As soon as particles were collected on the inner surface of the helix coil collector, the liquid samples were washed out rapidly and continuously with a stream of air to the outlet; their residence time was roughly 0.08-0.1 s. Khlystov *et al.* (1995) reported that even if the supersaturation of water vapor is only 10%, a residence time inside the mixing reservoir of about ~ 0.1 s is still sufficient for particles of 19 nm dry diameter to grow to 1 μm droplets.

The liquid samples were drained out after separation from the air stream in air/liquid separator and introduced into an online ion chromatography (IC) system. In air/liquid separator (Fig. 2c), the distance between the end of the outlet tube (Pyrex glass, 2 mm i.d.) and the wall surface was about 1 mm and the liquid samples were impacted on the wall surface. It was designed to minimize the loss of liquid droplets due to

(a) mixing part

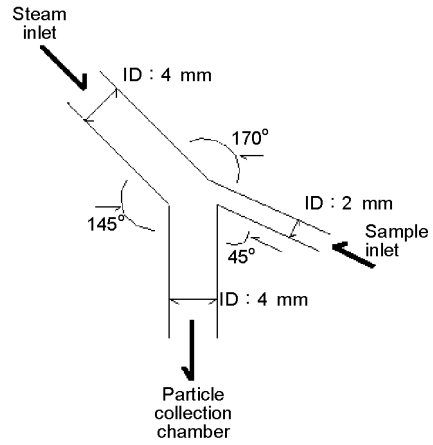

(b) particle collection chamber

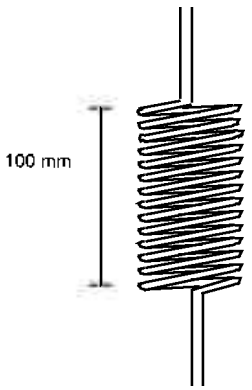

Inlet OD: 6.4 mm, ID: 4 mm, length: 80 mm
Coil tube OD: 6 mm, ID: 3 mm
Turns: 15, Coil length: 1750 mm.
Coil inner diam: 3 mm,
Coil outer diam: 3.8 mm
Outlet OD: 6.4 mm, ID: 4 mm, length: 80 mm

(c) air/liquid separator

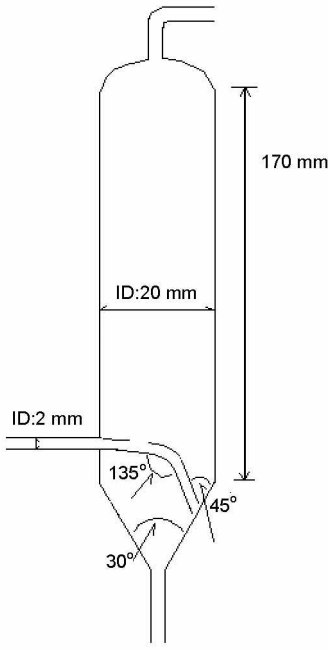

Figure 2. Details of the particle collection section: (a) mixing part (b) particle collection chamber (c) air/liquid separator.

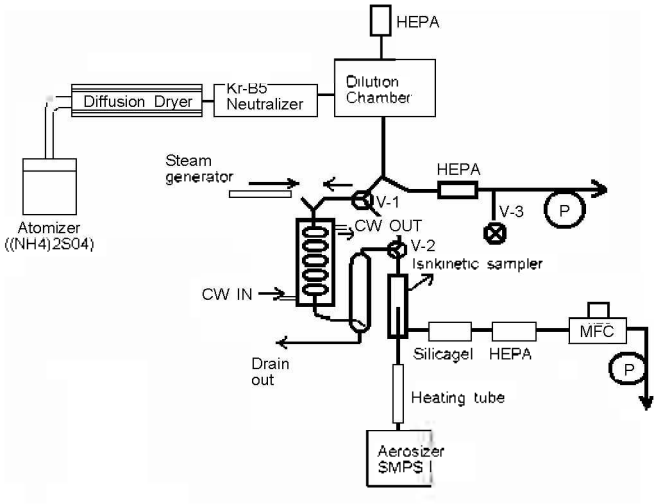

Figure 3. Schematic diagram of particle collection efficiency experiment (HEPA; HEPA filter, SMPS; Scanning Mobility Particle Sizer, DMA:TSI 3080 and CPC 3022, Aerosizer: API Inc., Model Mach II, MFC; mass flow controller, P; Air pump, V-1,2,3; 3-way valve, CW; Cooling water).

bounce-off on the glass wall surface and was intended to sample at the EPA standard sample flow rate of 16.7 L min^{-1}. All solutions were pumped through Teflon tubing (PTFE Microbore, ID: 0.022", OD: 0.042") using a low-flow and high-accuracy multichannel peristaltic pump (ISMATIC, A-95601-22).

Analytical system. The liquid samples were analyzed by two ion chromatography (IC) systems. Each IC system consisted of an automated time-controlled valve, set up with a sample loop, an analytical column, and a conductivity detector. The automated time-controlled valve (Rheodyne fluid processor Part No. 2320785C) was used to load liquid samples to the sample loops (500 μL) and then to inject them on to two analytical columns. Sample loops were employed for IC injection due to their simplicity and stability during field operations. In contrast, concentrator columns have been used in other techniques.[14,19] Cations were analyzed using a Shodex column (4 mm × 150 mm, YK-421) of a non-suppressor type. The analyses were carried out with an isocratic elution method using an eluent of a mixture of 2 mM HNO_3 and 0.75 mM dipicolinic acid (PDCA), at a flow rate of 1.0 mL min^{-1}. Anions were analyzed on a Dionex AS14-240 mm column, a chemical-suppressor type (50 mN H_2SO_4, flow rate 1.4 mL min^{-1}). This column was also operated with an isocratic elution method using an eluent of a mixture of 3.5 mM Na_2CO_3 and 1 mM $NaHCO_3$, at a flow rate of 1.2 mL min^{-1}. The liquid samples were introduced into the anion and cation sample loops in two six-way ports at a flow rate 0.17 mL min^{-1} (ISMATIC, A-95601-22), while pre-injected liquid samples were analyzed by the two IC systems. When the liquid samples were loaded into two sample loops, extra liquid samples with air bubbles were arranged to bypass through a simple de-bubbler. Approximately 20 min was required for a liquid sample to be quantified completely, due to the analytical time of the IC system. Peak areas were integrated with a NDA 401 Network Data Acquisition (Yullin Technology, Korea).

Calibrations were conducted after intensive field measurements over 2 weeks using standard solutions that were diluted from stock solutions (Exaxol Chemical Corporation, 05111B). In order to determine the air volume mixing ratios of aerosol components, it was crucial to accurately measure the flow rate of the air sample and the liquid volume for ambient aerosols dissolved in a particle collection section. LiBr was spiked into the distilled water used for steam generation to precisely calculate the liquid volume.[19] The flow rate of air samples was controlled using a rotameter, calibrated in the laboratory with a dry gas meter (Bios DryCal) prior to ambient air sampling.

Particle collection efficiency setup. Figure 3 shows a schematic diagram of the particle collection efficiency (PCE) setup. The size of tested aerosols ranged from 0.05 to 3.5 μm in aerodynamic diameter. As a performance test, a number of collection efficiencies experiments were conducted for various types of aerosols such as $(NH_4)_2SO_4$, NaCl, NH_4HSO_4, and NH_4NO_3. The test aerosols were generated by nebulizing the corresponding test aerosol liquid solutions using a Venturi-type nebulizer with dry, particle-free zero air, followed by their passage through a Kr-85 charge neutralizer. The concentrations of test aerosols are dependent on the concentration of the solution as well as the flow rate of carrier and dilution air. The dilution chamber allowed the mixing of test aerosols and particle-free air. The chemicals were of reagent grade (Merck) and deionized water was used for preparing solutions. For collection efficiency of test aerosols, the size distributions of the particles at the inlet and outlet of the particle collection section were measured by a SMPS system (Scanning Mobility Particle Sizer, DMA:TSI 3080 and CPC 3022) and an Aerosizer (API Inc., Model Mach II). The SMPS was used to measure the size distribution of small particles (< 0.5 μm) and the Aerosizer for larger particles (> 0.5 μm).

Experimental Results

Design of the air/liquid separator. Figure 4 illustrates the two types of air/liquid separator tested and Figure 5 indicates the collection efficiency (β) of the steam injected into the particle collection section, calculated as follows:

$$\text{CE } (\beta) \text{ of steam} = Q_2/Q_1 \times 100\ (\%), \quad (1)$$

where Q_1 is the water flow rate for generating the steam injected to the inlet of the Yconnector (0.65 mL min^{-1}) and Q_2 is

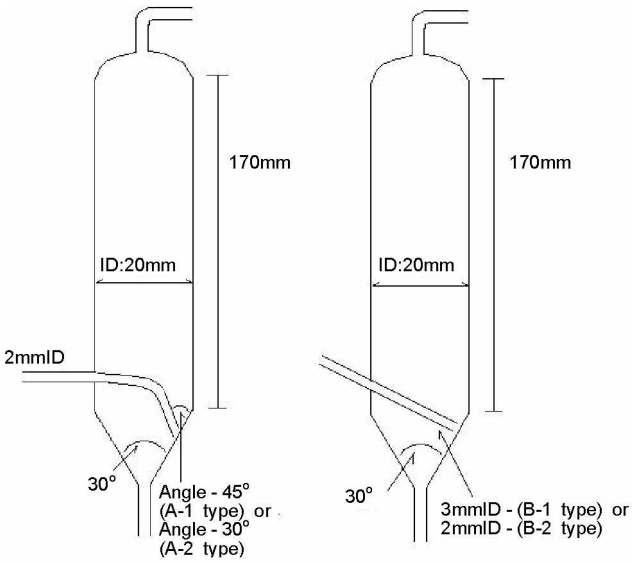

Figure 4. Various types of air/liquid separator (A-1, A-2, B-1, and B-2).

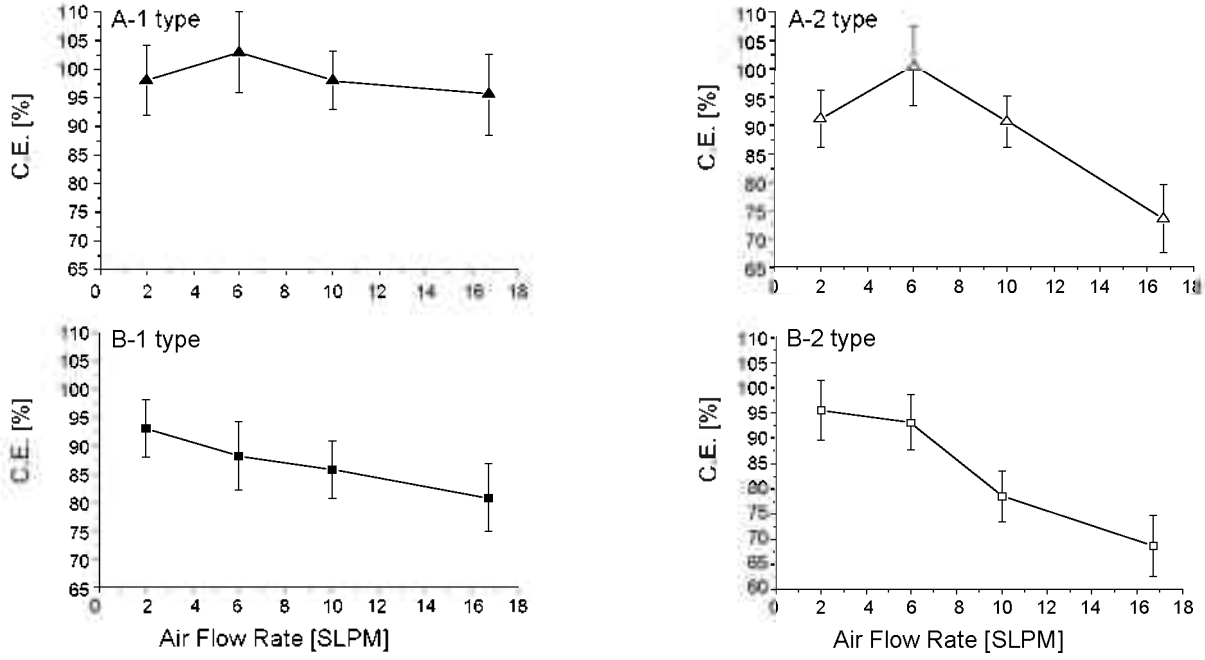

Figure 5. Collection efficiencies (β) of steams injected to particle collection section (▲:A-1 type, △:A-2 type, □: B-1 type, ■: B-2 type). Error bars mean one standard deviation (n = 5).

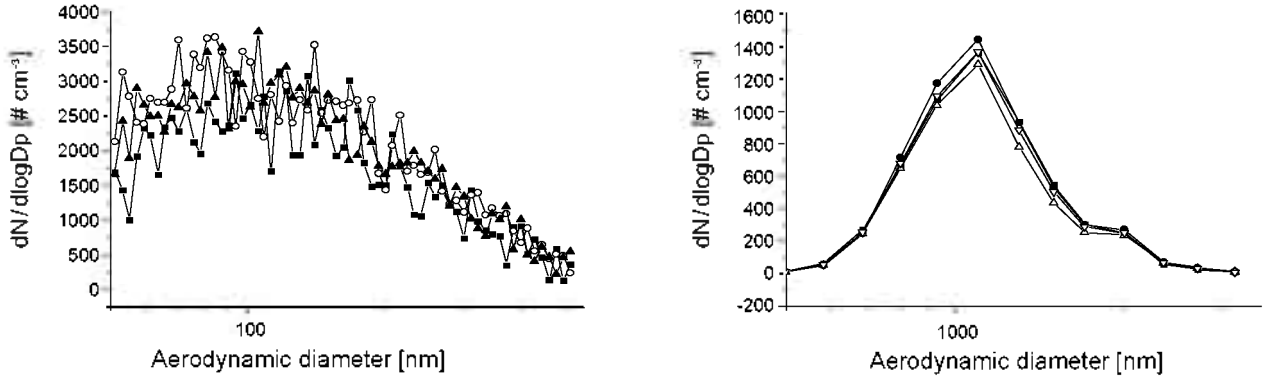

Figure 6. Size distributions of $(NH_4)_2SO_4$ tested in the range of 50-500 nm and over 500 nm in aerodynamic particle diameter.

the flow rate of liquids drained out in the air/liquid separator.

Figure 5 showed that β was similar at low air sample flow rates, but different at higher flow rates, depending on the design of the air/liquid separator. Except for the A-1 type, β decreased rapidly as the flow rate of the air sample increased. This decrease was mainly attributable to the combined effects of bounce-off on the wall surface, due to the impaction of liquid droplets, and the flow patterns of liquid droplets in the separator. In particular, these effects were more important at higher flow rates of air than a low flow rate. When liquid droplets were strongly impacted on the inner wall surface in the air/liquid separator, they bounced and then scattered, rather than draining out to the outlet. Consequently, this may have led to a decreased collection of steam in a given air/liquid separator. Furthermore, the liquid droplets after impaction could be advected with an air sample as the sample flow rate increased, especially when it was larger than 10 L min^{-1}. Thus, these effects must be considered in increasing β and an appropriate air/liquid separator design is required, especially at a high sample flow rate.

The results of this study indicated that β was larger than 95% in the A-1 design at 16.7 L min^{-1} (Fig. 5). The angle of the injection tube and the sliding surface in air/liquid separator was roughly 45° in the A-1 design (see Fig. 4). However, the results were not good when the A-2 design was applied, where the angle was about 30°, and β was less than 75% at 16.7 L min^{-1}. Although the bounce effect in the A-2 design was lower than in the A-1 design, as the sample flow rate increased, more liquid samples after impaction had a tendency to be transported together with the air sample. The bounce was greater in the B type due to its higher angle (i.e., 90°). When the response of the separator to the inner diameter was tested by using of 2 and 3 mm i.d. tube, liquid loss was almost entirely ascribed to the bounce effects. The β of the B-1 design (3 mm i.d. outlet tube) was better than that of the B-2 design (2 mm i.d. outlet tube) due to the smaller linear velocity.

Particle collection efficiencies. At a sample flow rate of 16.7 L min^{-1}, water flow rates for generating steam and number of coil turns of a particle collector were determined systematically through PCE tests to optimize the performance of the particle collection section. PCE tests were carried out by modifying number of coil turns (8 turns, 10 turns, 13 turns, and 15 turns) and the flow rates (0.17 mL min^{-1}, 0.35 mL min^{-1}, 0.65 mL min^{-1}, and 1.00 mL min^{-1}) of water injected for steam generation. In these experiments, the A-1 design of the air/liquid separator was used, as described above. PCEs of aerosols with diameters in the range of 50-500 nm and over 500 nm were calculated as follows:

$$PCEs = 1 - \sum C_{out} / \sum C_{in} \times 100\ (\%), \quad (2)$$

where C_{out} and C_{in} are the number concentrations of aerosol particles at the outlet and inlet of particle collection section, measured using a SMPS and an Aerosizer.

Figure 6 shows the size distributions of $(NH_4)_2SO_4$ tested in the range of 50-500 nm and over 500 nm upstream of the particle collection section. Figure 7 indicates size-resolved PCEs of the particle collection section in the range of 50-500 nm aerodynamic particle diameters at various water flow rates for steam generation and coil turns. The absolute uncertainties (S_y) of PCEs were calculated according to error propagation in multiplication or division as follows (n = 3):

$$(S_y)_r = \frac{S_y}{y} = \sqrt{(S_a)_r^2 + (S_b)_r^2 + (S_c)_r^2 \cdots},\ S_y = y \times (S_y)_r \quad (3)$$

where $(S_y)_r$ is the relative uncertainty and standard deviation divided by the mean value.[28] The resulting absolute uncertainties were found to be roughly of a magnitude of ±10%.

The results indicated that PCEs increased generally with an increased water flow rate for generating steam when the coil turns of a particle collector were constant. The PCEs were also observed to increase with the increasing number of coil turns at a constant flow rate for steam generation. These results were ascribed to the increased relative humidity and residence time, up to ~ 0.1 s. Figure 7 also shows the gradual increase in PCEs with increasing test aerosol size. The PCEs were 20-40% and 30-60% at water flow rates for steam generation of 0.17 and 0.35 mL min^{-1}, respectively. They increased up to ~ 80% with a particle collector of 15 turns, when the water flow rate for steam generation was 0.65 mL min^{-1}. As the water flow rate increased from 0.65 mL min^{-1} to 1.00 mL min^{-1}, the PCEs clearly increased from 40% to 60% with a particle collector of 8 turns, but were largely in the range of 70-80%.

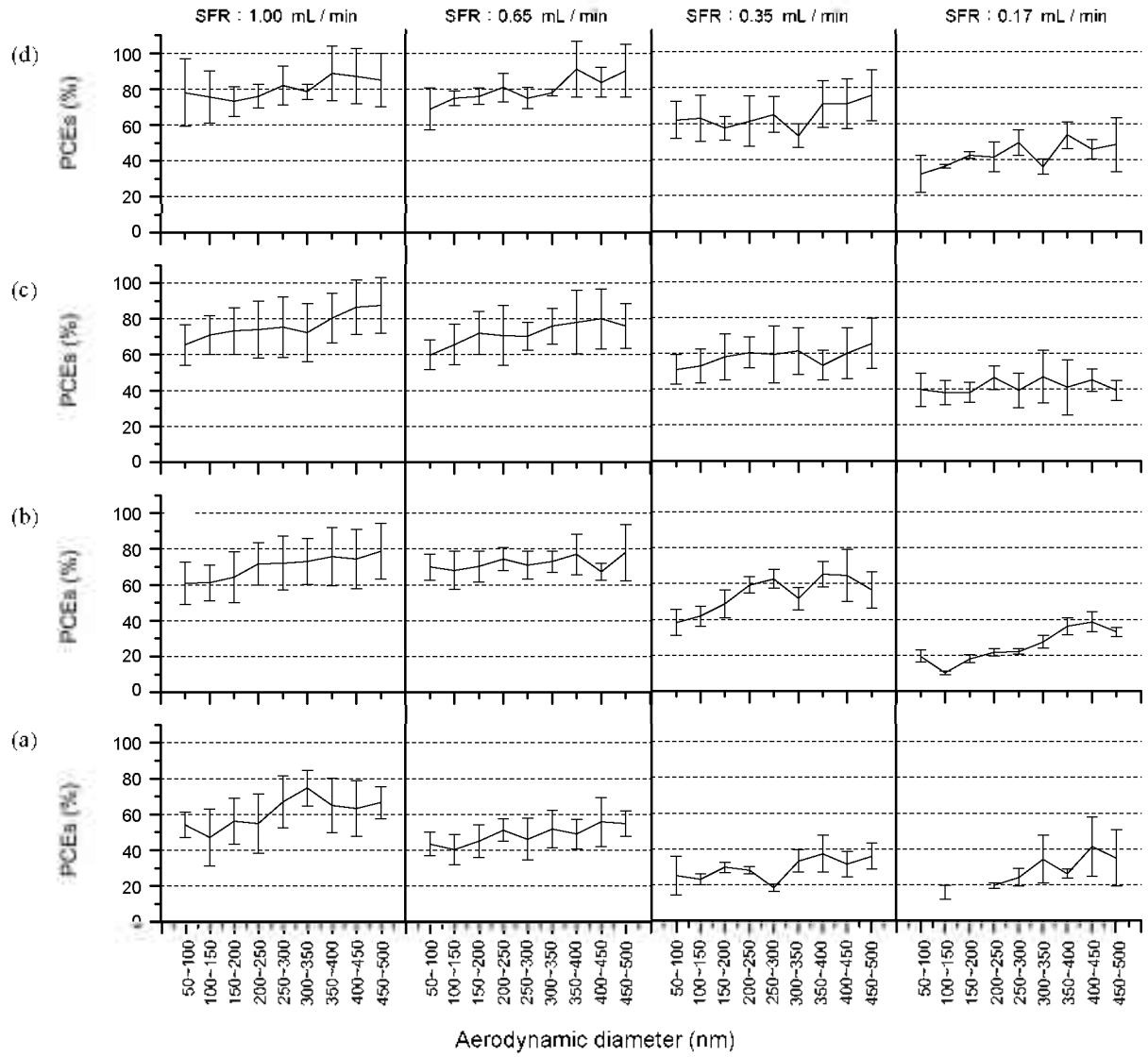

Figure 7. Size-resolved PCEs (%) of $(NH_4)_2SO_4$ in the range of 50-500 nm in aerodynamic particle diameter in the particle collection section according to DW flow rates for steam generation (SFR), measured by a SMPS (Scanning mobility particle sizer, DMA: TSI Mode 3080 and CPC: TSI Model 3020). (a; 8 turns, b; 10 turns, c; 13 turns, d; 15 turns, air flow rate: 2 L min^{-1}). Error bars indicates the absolute uncertainties of the PCEs (%).

with particle collectors of 10-15 turns.

In the range over 500 nm, the results were 50% and 90% at the air sample flow rate of 2 L min^{-1} and at the water flow rate of 0.17 mL min^{-1} for steam generation (see Fig. 8). The PCEs enhanced steadily up to 100% as the water flow rate increased from 0.17 to 1.00 mL min^{-1} at the sample flow rates lower than 6 L min^{-1}. Furthermore, the PCEs approached almost 100% when the sample flow rate was larger than 6 L min^{-1}, in the range of 0.17-1.00 mL min^{-1} for the water flow rate. The risk of a liquid droplet's loss on the inner surface of particle collector, due to turbulent deposition, was expected to increase as the Reynolds numbers increase at higher air sample flow rates.[29]

From the experimental results of PCEs above and the sensitivity of the system, a 15-turn coil particle collector and a steam flow rate of 0.65 mL min^{-1} were found to be optimal. Table 1 summarizes the PCEs of $(NH_4)_2SO_4$, NH_4NO_3, NaCl,

Table 1. The PCEs (%) for various test aerosols in particle collection section at 16.7 L min^{-1} (coil turns; 15 turns, steam flow rate; 0.65 mL min^{-1})

	Number Con. (# cm^{-3})	PCEs (%) (diam > 500 nm)	PCEs (%) (diam < 500 nm)
NaCl	63000	~100	90
	300000	~100	81
	780000	~100	57
$(NH_4)_2SO_4$	80000	~100	91
	350000	~100	80
	900000	~100	60
NH_4HSO_4	80000	~100	88
	300000	~100	64
	900000	~100	47
NH_4NO_3	70000	~100	88
	350000	~100	85

Table 2. The Reproducibilities (RSD, %), Linearities (r^2), and Limits of Detection (LOD) of semicontinuous ion measurement system during field measurement period.

NO	Components	Reproducibility (RSD[a], %)	Linearity (r^2)	LOD[b] ($\mu g\ m^{-3}$)
1	Cl^-	11.4 at 10 ppb	0.92 ~ 0.99	0.06 ~ 0.25
2	NO_2^-	16.0 at 10 ppb	0.94 ~ 0.99	0.06 ~ 0.25
3	NO_3^-	24.0 at 5 ppb	0.94 ~ 0.99	0.06 ~ 0.25
4	SO_4^{2-}	5.0 at 15 ppb	0.98 ~ 0.99	0.06 ~ 0.25
5	Na^+	4.0 at 20 ppb	0.99 ~ 0.99	0.25 ~ 0.50
6	NH_4^+	4.5 at 40 ppb	0.98 ~ 0.99	0.24 ~ 0.50
7	K^-	14.3 at 20 ppb	0.98 ~ 0.99	0.13 ~ 0.28
8	Mg^{2+}	15.1 at 20 ppb	0.97 ~ 0.99	~ 0.20
9	Ca^{2+}	25.0 at 10 ppb	0.97 ~ 0.99	~ 0.20

[a]Relative standard deviation (standard deviation/mean 100) [b]LOD was calculated as the three times of noise level of system blank at 99% confidence level

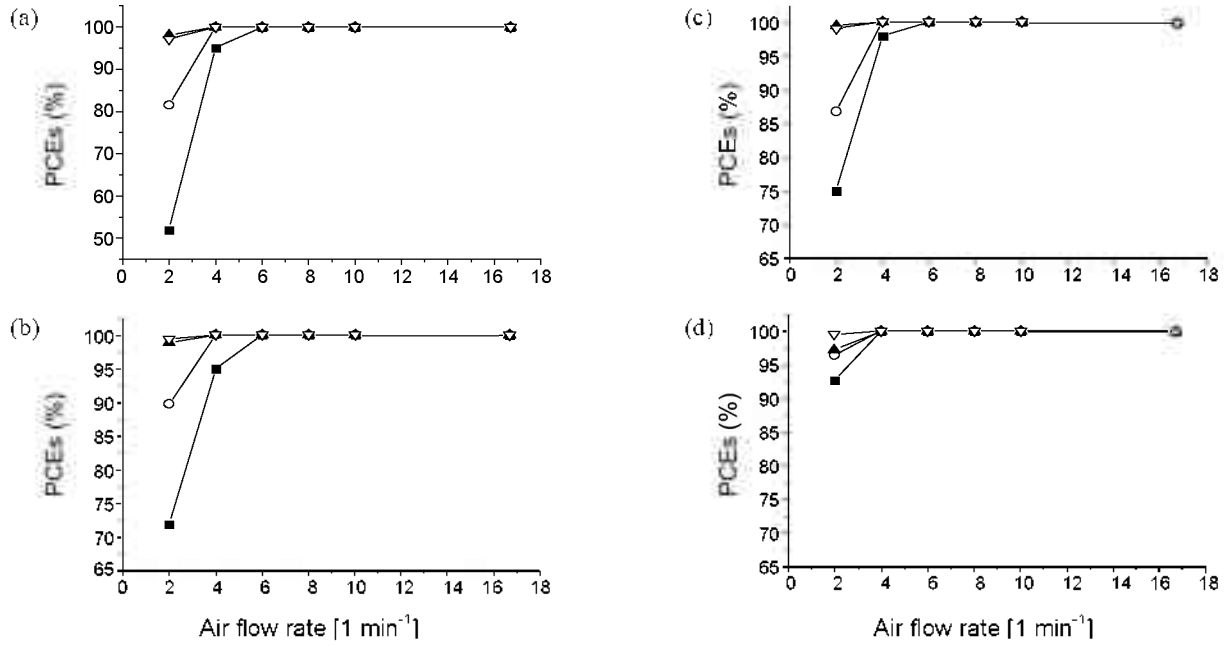

Figure 8. PCEs (%) of $(NH_4)_2SO_4$ in the Particle collection section (particle diam > 500 nm) (water flow rates for steam generation: ■:0.17 mL min^{-1}, ○:0.35 mL min^{-1}, ▲:0.65 mL min^{-1}, ▽:1.00 mL min^{-1}) (a) 8 turns, (b) 10 turns, (c) 13 turns, (d) 15 turns.

and NH_4HSO_4 at various concentrations. The results indicated that the PCEs were almost 100% in the range over 500 nm at different concentrations. However, the PCEs were 50-90% for particles in the range of 50-500 nm, depending on types of test aerosols and their number concentrations. In particular, they decreased gradually as the concentrations of test aerosols increased; the higher the number concentration of test aerosols was, the more difficult it was to induce growth of the test aerosols at constant steam flow rates. In the case of test aerosols less than 500 nm, the lowest number concentrations tested were comparable to real urban areas, such as Seoul, Korea.[30-31] Thus, the PCEs (88-91%) of these concentration levels were meaningful in terms of the field campaign.

Field observations of $PM_{2.5}$ soluble species. A field campaign was conducted at an atmospheric observatory located on Mt. Muak, on January 11-24, 2006, at Yonsei University (sea level: ~250 m) in Seoul. A major road was adjacent to the measurement site, 30 m to the northeast. The $PM_{2.5}$ cyclone of measurement system was set up on the roof of trailer (4 m above the ground surface). The denuder systems were replaced every 3-4 days. The reproducibility (RSD, %), linearity (r^2), and limits of detection (LOD) of system in the field experiment are shown in Table 2.

The reliability of analytical data was examined by the ion charge balance theory of soluble inorganic species in aerosol particles. According to this theory, the sum of the cation equivalent concentrations should be identical to the sum of the anion equivalent concentrations if all soluble ions in aerosol particles are accurately analyzed. Thus, this theory can be used to verify accurate determination of the major ionic species. Figure 9 shows scattergrams between the sum of the cation equivalent concentrations and the sum of the anion equivalent concentrations. According to the result of the regression analysis, the Pearson correlation coefficient was 0.87 with the uncertainties of 95% confidence intervals. The slope (1.3) of the regression line indicated that the sum of the cation

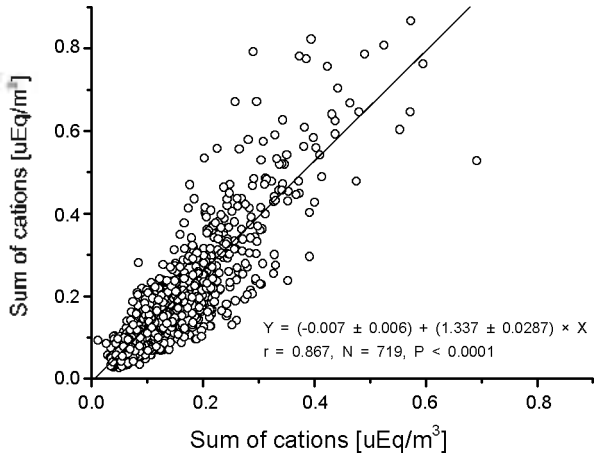

Figure 9. Ion charge balance for the measured inorganic species in $PM_{2.5}$. (Cations: $Ca^{2-} + Mg^{2-} + K^- + Na^- + NH_4^+$, Anions: $Cl^- + NO_2^- + SO_4^{2-}$).

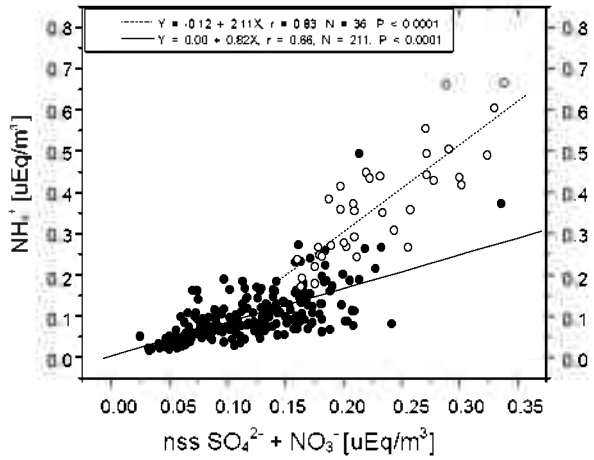

Figure 10. The scattergrams between NH_4^+ and nss-SO_4^{2-} + NO_3^-. (○: Jan. 15, 10:00 - Jan. 16, 18:00 ●: others).

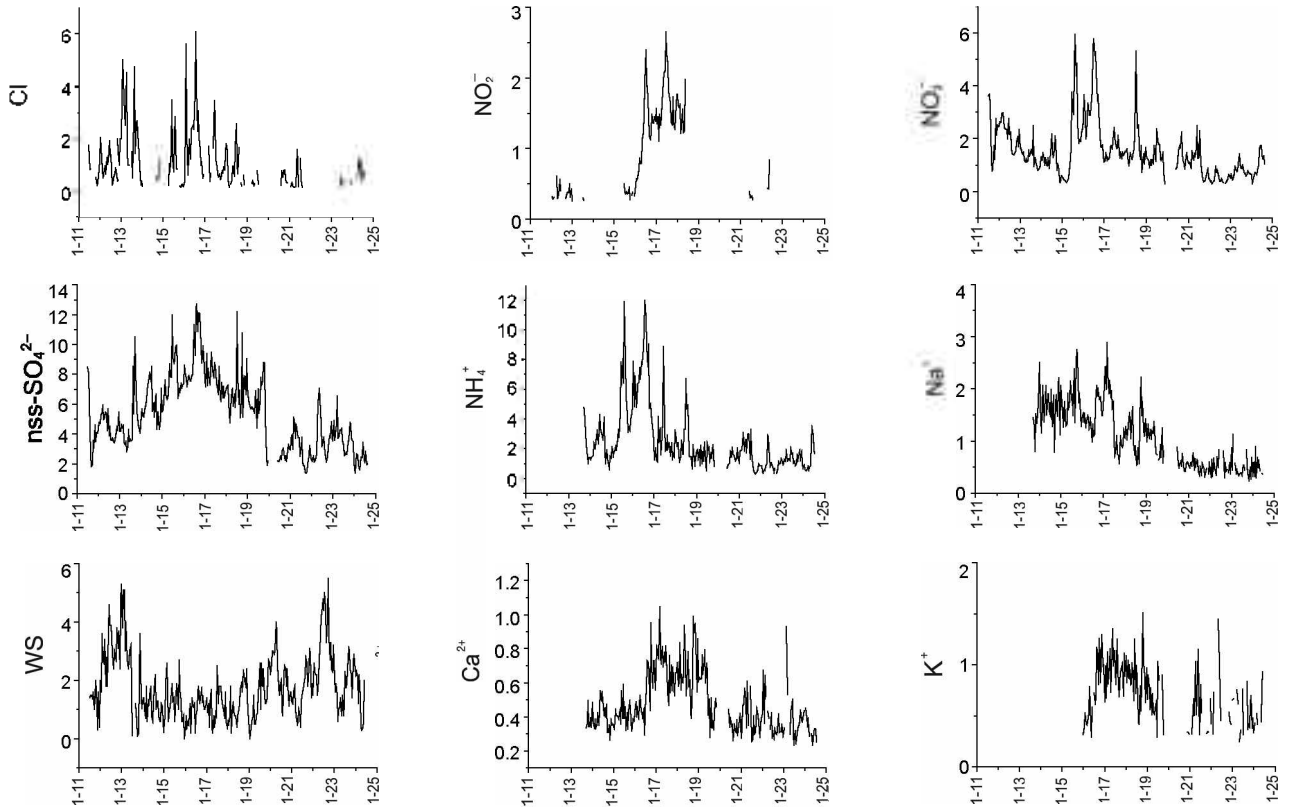

Figure 11. Time series of inorganic species in $PM_{2.5}$ and wind speed (WS) measured during field campaigns (unit of inorganic species: μg m^{-3}, unit of WS: m sec^{-1}, Rainfall event: 20:00 h, Jan. 12 ~ 16:00 h, Jan. 13, the maximum rainfall: 5 mm on 06:00, Jan. 13). The anion eluent delivery pump got out of order on 00:00 ~ 10:00 h, Jan 20.

equivalent concentrations was somewhat larger than that of the anion equivalent concentrations. There may be several possible reasons why we underestimated anion species and overestimated cation species. The contributions of organic anions such as $HCOO^-$ and CH_3COO^- may be small because their concentrations were even lower than those of acidic anions, such as SO_4^{2-} and NO_3^-. The contribution of CO_3^{2-}, which was not determined in IC, was also unlikely to be significant, due to its dominant existence of $CaCO_3$ in the coarse mode (2.5 < diameter < 10 μm) of aerosols.[32,33] The determinations of Na^- and NH_4^- with uncertainties took placed frequently owing to the overlap of the two peaks in IC chromatograms. Figure 10 indicates that the slope of the regression line between NH_4^- and $2SO_4^{2-} + NO_3^-$ was ~ 0.8 in the low concentration ranges, but ~ 2 in higher concentration ranges. Thus, NH_4^- in particular may be overestimated at higher concentration ranges. This may also contribute to bias the slope of the total data.

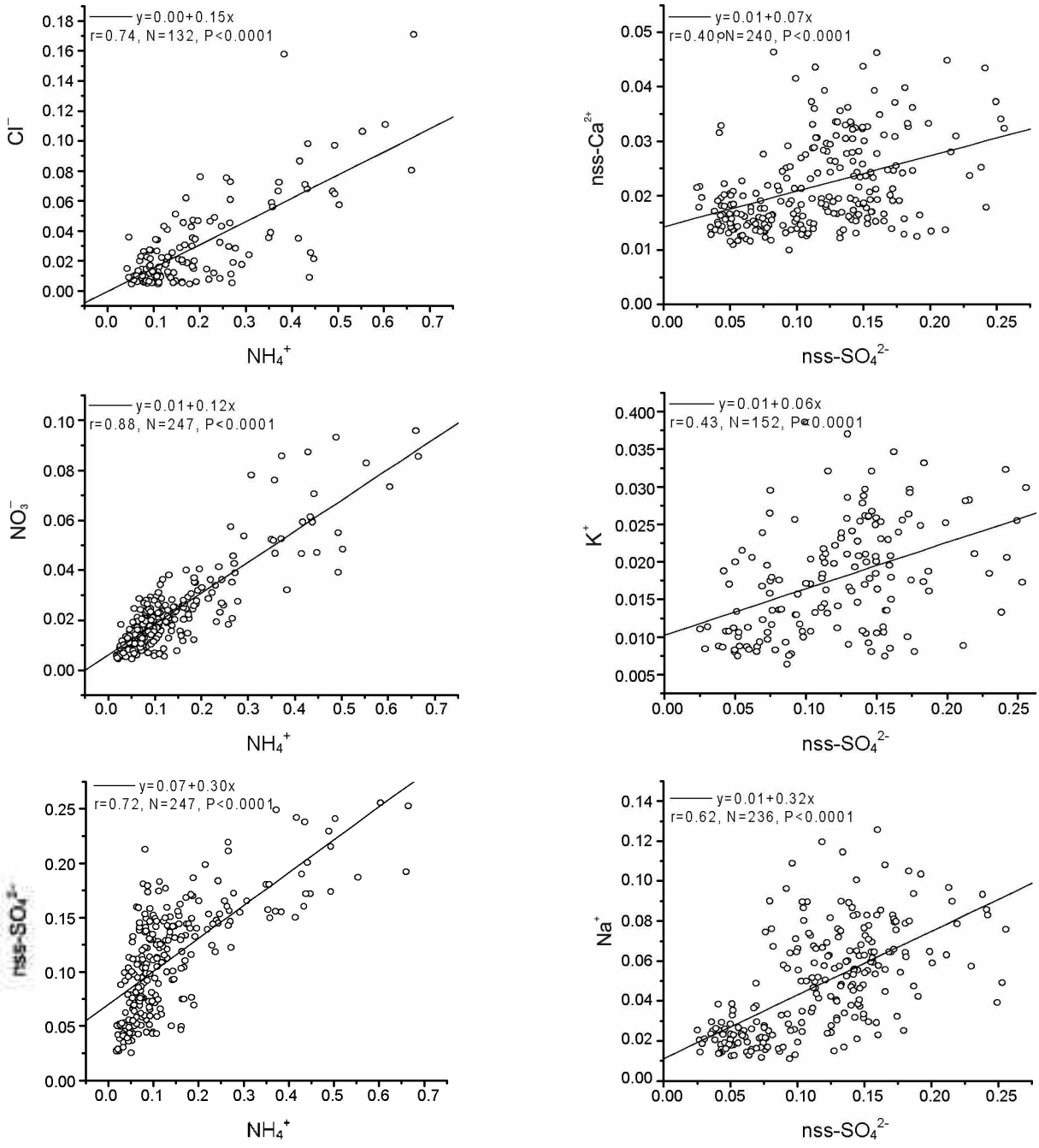

Figure 12. Scattergrams between major cationic species and anionic species (unit; uEq m^{-3}).

Figure 11 illustrates the temporal variations in ionic species in $PM_{2.5}$ and the wind speed (WS) during the measurement period. The concentrations of NH_4^+, Na^+, K^+, Ca^{2+}, SO_4^{2-}, NO_3^-, NO_2^-, and Cl^- were 2.52 ± 2.18 (±standard deviation), 1.09 ± 0.61, 0.70 ± 0.33, 0.48 ± 0.17, 5.37 ± 2.46, 1.53 ± 1.02, 0.98 ± 0.64, and 1.04 ± 0.98 μg m^{-3}, respectively. Generally, the levels of ionic species in $PM_{2.5}$ remained relatively low until January 15 and increased steadily thereafter. In particular, the concentrations of NH_4^+, SO_4^{2-}, and NO_3^- clearly began to increase from January 15 and those of K^+, NO_2^-, and Ca^{2+} increased from January 16. Their concentrations again decreased in the late afternoon on January 19 and then remained low. Figure 11 indicates that the concentrations of anions and paired cations varied generally with similar trends. Figure 12 illustrates the relationships between paired ions. Correlation coefficients indicated that the main forms of the compounds in $PM_{2.5}$ were $(NH_4)_2SO_4$, Na_2SO_4, NH_4Cl, and NH_4NO_3, but that some K_2SO_4 and $CaSO_4$ were also present.

The distributions of the ionic species in $PM_{2.5}$ are primarily influenced by photochemistry, thermodynamics, and meteorology.[24,25,34] The contribution of photochemical processing was expected to be minor because of the generally low temperature (maximum temperature: ~ 8 °C), low levels of photochemical oxidants (maximum levels of O_3: ~ 25 ppbv), and weak radiation in the daytime during the winter. The relationships between photochemical products (nss-SO_4^{2-} and

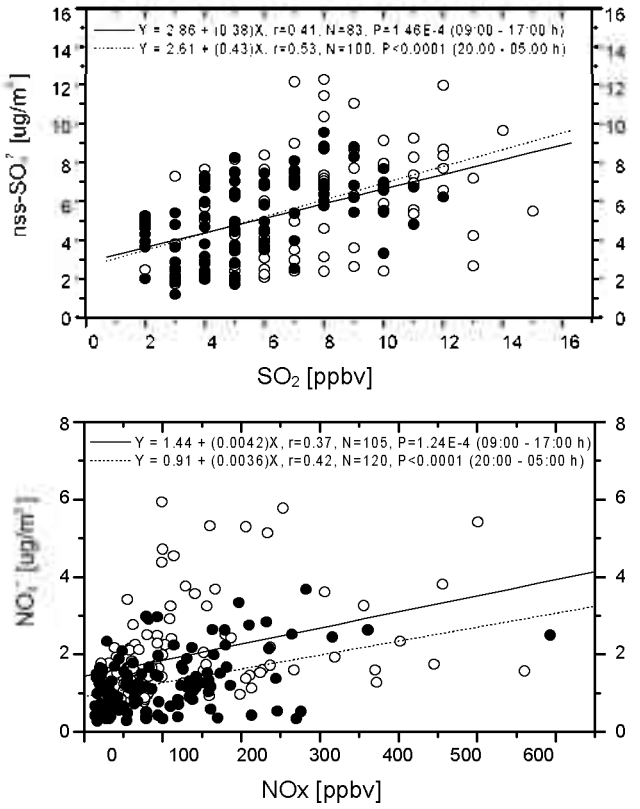

Figure 13. The scattergrams between secondary species (nss-SO_4^{2-}, NO_3^-) in fine particles and precursor gases (SO_2, NOx) (Data influenced by fresh emissions from vehicles were removed).

NO_3^-) in particles and precursor gases (SO_2 and NOx) were investigated (see Fig. 13). The results indicated that the secondarily formed ions in $PM_{2.5}$ were weakly associated with their precursors, and their concentration ratios (slopes) were also similar during both day and nighttime. Thus, the photochemical formation paths of nss-SO_4^{2-} and NO_3^- in aerosols were unimportant.

Semi-volatile species, such as NH_4NO_3 and NH_4Cl, in $PM_{2.5}$ can be present in the forms of gaseous precursors and/or the particle phase, depending on their thermodynamic properties. In general, they are primarily in the particle phase at 08:00-09:00 h in the morning, when the temperature is typically lowest, and then in the gaseous precursors in the daytime as the temperature increases. However, in this study, the transition to gaseous precursors in the daytime may not have occurred because the maximum temperature was only about 8 °C. As a result, the concentrations of NO_3^- and Cl^- did not show higher levels in the nighttime. On the contrary, the maximum levels of NO_3^- were observed frequently in the daytime as follows: 15:00 h (January 13), 12:00-16:00 h (January 14), 15:00 h (January 15), 12:00 h (January 16), 11:00 h (January 17), 12:00 h (January 18), 12:00 h (January 19), 16:00 h (January 20), 13:00 h (January 21), and 12:00 h (January 23) (see Fig. 11).

The relationships between concentrations of species and meteorological parameters, such as rainfall and WS, were investigated. It rained from 20:00 h, January 12 to 16:00 h, January 13 and the maximum rainfall was 5 mm on 06:00,

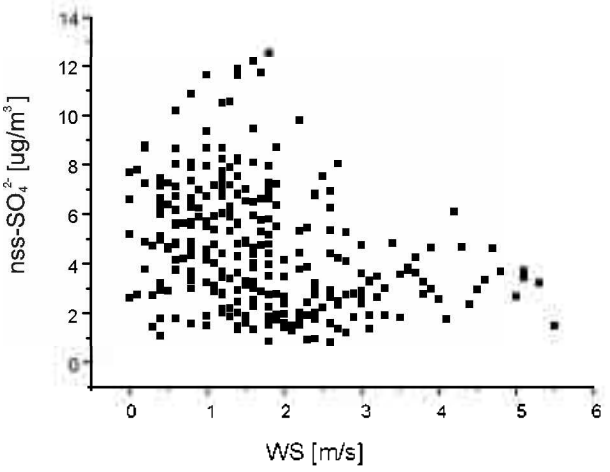

Figure 14. The scattergrams of wind speed (WS) and SO_4^{2-} in $PM_{2.5}$.

January 13. Even though it rained on January 12-13, the washout effect was low because the intensity of rain was weak and no correlation was detected between rainfall and the levels of $PM_{2.5}$ ionic species. It is to be noted that the WS was anti-correlated with levels in $PM_{2.5}$ (Fig. 11). Generally, WS increased in the daytime and decreased at night during the measurement period. It was about ~ 1 m s^{-1} on January 12 and then steadily increased to 5 m s^{-1}. Thereafter, it abruptly decreased at dawn on January 13. It maintained 1-2 m s^{-1} until January 18, and increased again in the afternoon of January 19. The WS approached ~ 5 m s^{-1} as a maximum in the daytime on January 22 and then decreased. These results showed a reverse trend to the levels of $PM_{2.5}$, which were very low, especially on January 13 and January 20 when the WS was about 5 m s^{-1}. Furthermore, the levels of $PM_{2.5}$ were generally higher when the WS was relatively lower from January 14 to 18. Figure 14 shows scattergrams of WS and SO_4^{2-} in $PM_{2.5}$. SO_4^{2-} is thermodynamically stable, compared to the other ionic species, and thus its distributions are frequently controlled by the meteorological processes such as dispersion and advection of $PM_{2.5}$. The results clearly indicated that SO_4^{2-} levels were negatively correlated with WS. That is, as WS increased, the SO_4^{2-} in $PM_{2.5}$ decreased. These results showed that the concentrations of ionic species in $PM_{2.5}$ were closely associated with WS and the pollutants were dispersed actively as WS increased during the measurement period.

Conclusions

An instrument was developed to semicontinuously determine $PM_{2.5}$ ionic species. It has a shorter time resolution (20 min), compared to instruments using filter methods, and operated best at a sample flow rate of 16.7 L min^{-1}. The particle collection section (mixing part, particle collection chamber, and air/liquid separator) was developed and optimized by sensitivity analyses of the PCEs using various types of test aerosols. The absolute uncertainties of size-resolved PCEs of the particle collection section in the range of 50-500 nm aerodynamic particle diameter were found to be roughly of a magnitude of ± 10% at various water flow rates for steam

generation and coil turns. The PCEs were almost 100% at different concentration levels in the range over 500 nm in diameter but 50-90% in the range of 50-500 nm under the following experimental conditions: 15 coil turns, a water flow rate for steam generation of 0.65 mL min^{-1}, and an air sample flow rate of 16.7 L min^{-1}. This technique was applied to field measurements of the chemical compositions of $PM_{2.5}$ during January 11-24, 2006, at Yonsei University in Seoul, Korea. The results indicated that SO_4^{2-} and NH_4^+ in $PM_{2.5}$ were present at high levels from January 15 to 19. Regression analyses between ions in $PM_{2.5}$ showed that $(NH_4)_2SO_4$, Na_2SO_4, NH_4Cl, and NH_4NO_3 were the major components. The concentrations of $PM_{2.5}$ ionic species during the measurement periods were influenced by a number of processes such as thermodynamics, photochemical conversions, and meteorological transport. Of the processes, meteorological transport appeared to play the most important role in the variations of the ionic species.

Acknowledgments. This work was supported in part by the Brain Korea 21 Project, and by the Korea Science and Engineering Foundation (KOSEF) through the Advanced Environmental Monitoring Research Center (ADEMRC) at Gwangju Institute of Science and Technology (GIST). And this work was also supported in part by a research grant (PP09010) from the Korean Research Council of Public Science and Technology. The authors greatly acknowledge Prof. D. S. Lee and Prof. B. K. Lee (Yonsei University) for their supports during field measurement period. The authors wish to thank Korea Meteorological Administration (KMA) for supporting the meteorological data.

References

1. Charlson, R. J.; Schwartz, S. E.; Hales, J. M.; Cess, R. D.; Coakley, J. A.; Hansen, Jr., J. E.; Hofmann, D. J. *Science* **1992**, 255, 423.
2. Cass, G. R. *Atmospheric Environment* **1979**, *13*, 1069.
3. Jacob, D. J. *Atmospheric Environment* **2000**, *34*, 2131.
4. Dockey, D. W.; Pope, C. A. *Annu. Rev. Public Health* **1994**, *15*, 107.
5. Albrecht, B. A. *Science* **1989**, *245*, 1227.
6. Fowler, D.; Cape, J. N.; Sutton, M. A.; Mourne, R.; Hargreaves, K. J.; Duyzer, J. H.; Gallagher, M. W. In *Acidification Research: Evaluation and Policy Applications*; Proc. Int. Conf, 1992; p 553.
7. *On Res. Priorities for airborne particulate matter*; National Research Council (NRC): Washington, D. C., 1998.
8. Slanina, J.; ten Brink, H. M.; Otjes, R. P.; Even, A.; Jongejan, P.; Khlystov, A.; Waijers-Ijpelaan, A.; Hu, M.; Lu, Y. *Atmospheric Environment* **2001**, *35*, 2319.
9. Chow, J. C. *Journal of Air and Waste Management* **1995**, *45*, 320.
10. Buhr, S.; Buhr, M. P.; Fehsenfeld, F. C.; Holloway, J. S.; Karst, U.; Norton, R. B.; Parrish, D. D.; Sievers, R. E. *Atmospheric Environment* **1995**, *29*(1), 2609.
11. Khlystov, A.; Wyers, G. P.; Slanina, J. *Atmospheric Environment* **1995**, *29*, 2229.
12. Simon, P. K.; Dasgupta, P. K. *Analytical Chemistry* **1995**, *67*, 71.
13. Liu, S.; Dasgupta, P. K. *Analytical Chemistry* **1996**, *68*, 3638.
14. Weber, R.; Orsini, D.; Daun, Y.; Lee, Y. N.; Klotz, P. J.; Brechtel, F. *Aerosol Science and Technology* **2001**, *35*, 718.
15. Boring, C. B.; Al-Horr, R.; Genfa, Z.; Dasgupta, P. K.; Martin, M. W.; Smith, W. F. *Analytical Chemistry* **2002**, *74*, 1256.
16. Al-Horr, R.; Samanta, G.; Dasgupta, P. K. *Environmental Science and Technology* **2003**, *37*, 5711.
17. Hinds, W. C. *Aerosol Technology: Properties, Behaviors, and Measurement of Airborne Particles*; John Wiley & Sons: 1982; p 214.
18. Seinfeld, J.; Pandis, S. *Atmospheric Chemistry and Physics: From Air Pollution to Climate Change*; Wiley-interscience: New York, 1998; p 355.
19. Orsini, D. A.; Ma, Y.; Sullivan, A.; Sierau, B.; Baumann, K.; Weber, R. J. *Atmospheric Environment* **2003**, *37*, 1243.
20. Maxwell-Meier, A.; Weber, R.; Song, C.; Orisi, D.; Ma, Y.; Carmichael, G. R.; Streets, D. G. *Journal of Geophysical Research* **2004**, *109*, D19S07.
21. URG operation manual; *Use and Maintenance of URG Annular Denuders* **2000**, 25.
22. Park, S. S.; Hong, S. B.; Jung, Y. G.; Lee, J. H. *Atmospheric Environment* **2004**, *38*, 293.
23. Lee, J. H.; Y. Chen, I.; Tang, N. *Environmental Science and Technology* **1991**, *25*, 339.
24. Kim, Y. P.; Seinfeld, J. H.; Saxena, P. *Aerosol Science and Technology* **1993a**, *19*, 157.
25. Kim, Y. P.; Seinfeld, J. H.; Saxena, P. *Aerosol Science and Technology* **1993b**, *19*, 182.
26. Kim, D. S.; Lee, D. S.; Woo, C. G.; Choi, M. *Journal of Aerosol Science* **2006**, *37*, 1876.
27. Kim, D. S.; Kang, C. H.; Hong, S. B.; Lee, K. W.; Lee, J. H. *Journal of Korean Society for Atmospheric Environment* **2008**, *24*(E1), 24.
28. Skoog, D. A.; West, D. M.; James Holler, F.; Crouch, S. R. *Analytical Chemistry: An introduction*; Brooks/Cole: 2000; p 140.
29. Hinds, W. C. *Aerosol Technology: Properties, Behaviors, and Measurement of Airborne Particles*; John Wiley & Sons: 1982; p 24.
30. Chun, Y. S.; Kim, J. Y.; Choi, J. C.; Boo, K. O.; Oh, S. N.; Lee, M. H. *Atmospheric Environment* **2001**, *35*, 2715.
31. Bae, G. N.; Kim, M. C.; Lim, D. Y.; Moon, K. J.; Baik, N. J. *Journal of Korean Society for Atmospheric Environment* **2003**, *19*(2), 167.
32. Song, C. H.; Carmichael, G. R. *Atmospheric Environment* **1999**, *33*, 2203.
33. Song, C. H.; Carmichael, G. R. *Journal of Geophysical Research* **2001**, *106*, 18131.
34. Hong, S. B.; Kim, D. S.; Ryu, S. Y.; Kim, Y. J.; Lee, J. H. *Atmospheric Research* **2008**, *89*, 62.